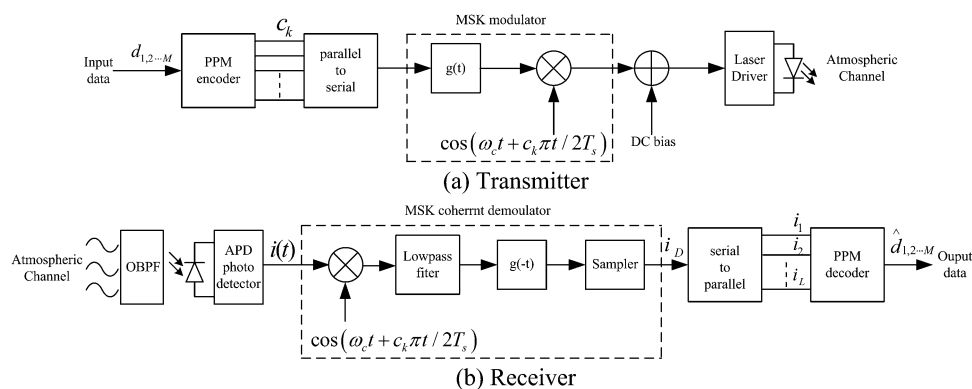


# BER Analysis of a Hybrid Modulation Scheme Based on PPM and MSK Subcarrier Intensity Modulation

Volume 7, Number 4, August 2015

Hongzhan Liu  
Renbo Liao  
Zhongchao Wei  
Zhiyun Hou  
Yaojun Qiao



# BER Analysis of a Hybrid Modulation Scheme Based on PPM and MSK Subcarrier Intensity Modulation

Hongzhan Liu,<sup>1,2</sup> Renbo Liao,<sup>1</sup> Zhongchao Wei,<sup>1</sup>  
Zhiyun Hou,<sup>1</sup> and Yaojun Qiao<sup>2</sup>

<sup>1</sup>Guangdong Provincial Key Laboratory of Nanophotonic Functional Materials and Devices, South China Normal University, Guangzhou 510006, China

<sup>2</sup>State Key Laboratory of Information Photonics and Optical Communications, Beijing University of Posts and Telecommunications, Beijing 100876, China

DOI: 10.1109/JPHOT.2015.2449265

1943-0655 © 2015 IEEE. Translations and content mining are permitted for academic research only.

Personal use is also permitted, but republication/redistribution requires IEEE permission.

See [http://www.ieee.org/publications\\_standards/publications/rights/index.html](http://www.ieee.org/publications_standards/publications/rights/index.html) for more information.

Manuscript received May 31, 2015; accepted June 20, 2015. Date of publication June 24, 2015; date of current version July 7, 2015. This work was supported in part by the National Basic Research Program of China under Grant 2013CB29204 and in part by the National Natural Science Foundation of China under Grant 61475049. Corresponding author: R. Liao (e-mail: renboliao@m.scnu.edu.cn).

**Abstract:** In order to improve the bit-error-rate (BER) performance of free-space optical (FSO) communication systems employing binary phase-shift keying subcarrier intensity modulation (BPSK-SIM), an innovative hybrid modulation scheme called PPM-MSK-SIM is proposed, which is based on pulse position modulation (PPM) and minimum shift keying (MSK) subcarrier intensity modulation. Subsequently, the BER performance of PPM-MSK-SIM is studied in detail for an FSO system over log-normal turbulence channels with avalanche photodiode detection. The results of the numerical simulation show that PPM-MSK-SIM has the advantages of improving the BER performance compared with BPSK-SIM and PPM. For example, at the same received irradiance of  $-2.1$  dBm and the same strength of turbulence  $C_n^2 = 7.5 \times 10^{-15} \text{ m}^{-2/3}$ , the BER performance of 2-PPM-MSK-SIM can decrease to  $1.02 \times 10^{-9}$ , whereas those of 2-PPM and BPSK-SIM are just  $1.19 \times 10^{-7}$  and  $2.29 \times 10^{-6}$ , respectively. This makes PPM-MSK-SIM a favorable candidate for the modulation technique in FSO communication systems.

**Index Terms:** Free-space optical communication, subcarrier intensity modulation, atmospheric turbulence, atmospheric attenuation, bit-error rate (BER).

## 1. Introduction

Free space optical (FSO) communication has many significant advantages, such as large transmission capacity, high transmission rate, and good immunity to electromagnetic interference [1]–[4]. However, the bit-error rate (BER) performance of FSO systems is highly susceptible to adverse atmospheric conditions. One of the major factors under clear air conditions is atmospheric turbulence, which is caused by inhomogeneities of both temperature and pressure variation, and is responsible for the refractive index variation of the air [5]–[8]. Thus, the atmospheric turbulence lead to severe degradation of signal optical intensity at the receiver, increase the BER, and even break the communication link [8]. For different atmospheric turbulence intensity, in recent years, a number of statistical models have been introduced. For example, lognormal, gamma-gamma, and negative exponential models are the most commonly used for the cases of weak-to-moderate,

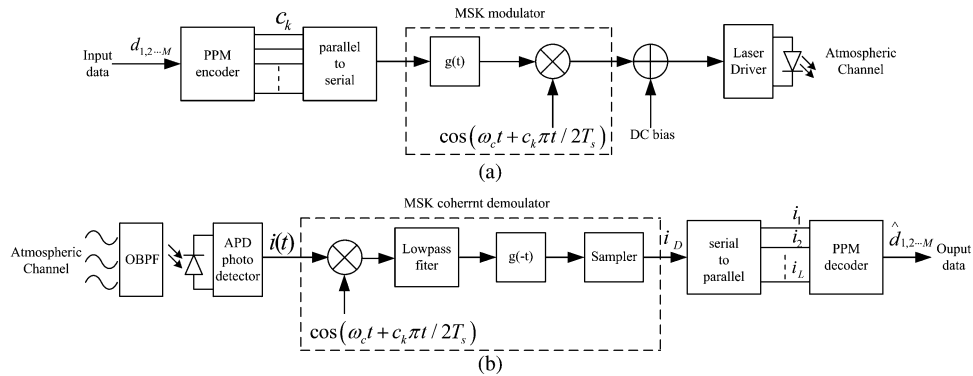


Fig. 1. Block diagram of FSO communication systems using PPM-MSK-SIM. (a) Transmitter end and (b) receiver end.

moderate-to-strong, and saturated turbulence channels, respectively [7]–[12]. To overcome the challenges of atmospheric turbulence, one of the main factors in the implementation of high performance FSO systems is the modulation technique. Under the premise of high transmission rate and low BER, by choosing one appropriate modulation scheme and the corresponding demodulation technology will reduce the affects of atmospheric turbulence on the FSO communication.

Conventionally, on-off keying (OOK) based on intensity modulation/direct detection (IM/DD) is the most widely adopted modulation scheme thanks to its simple implementation and low cost [3]. But FSO systems employing OOK has been found to be sub-optimal over atmospheric turbulence channels [13]–[15]. Then, the pulse position modulation (PPM) has been used widely in FSO communication systems. However, the bandwidth efficiency of PPM is poor, and it needs symbol synchronization [3], [15]. As a potential alternative to the OOK is subcarrier intensity modulation (SIM), which was first proposed for FSO systems by Huang *et al.* in [16]. Thereafter, the performance of subcarrier binary phase shift keying (BPSK) intensity modulation FSO systems has been extensively studied in [9]–[11], [17]–[20]. As we all know, compared with the traditional SIM in FSO communication systems, the BER performance of BPSK-SIM is superior over the other modulation schemes such as MPSK, QPSK, DPSK, QAM and so on [20]–[22].

For further improving the BER performance of FSO systems employing BPSK-SIM, in this paper, an innovative hybrid modulation scheme called PPM-MSK-SIM is proposed, which is based on PPM and MSK subcarrier intensity modulation. Then the BER performance of PPM-MSK-SIM is theoretically analyzed, verified using simulated data and compared with BPSK-SIM and PPM over lognormal turbulence channels for an avalanche photodiode (APD) detection scheme. The rest of the paper is organized as follows. In Section 2, we introduce the configuration of FSO communication system with PPM-MSK-SIM and its corresponding theory. In Section 3, we describe the channel models with atmospheric turbulence and attenuation. In Section 4, we analyze the BER performance of the proposed modulation scheme over the lognormal turbulence channels. Numerical results and discussions are presented in Section 5. Finally, conclusions are given in Section 6.

## 2. FSO Communication System With PPM-MSK-SIM

For an FSO communication system, the PPM-MSK-SIM can be described as follows: First, a block of  $M = \log_2 L$  data bits is converted into the symbol format of PPM, here,  $M$  is the number of bits per symbol or the modulation order, and  $L$  is the average length of symbol; second, the PPM codeword will become a new array of data after a parallel-to-serial conversion; finally the new array of data is modulated into the subcarrier signal using the MSK signal. The configuration of PPM-MSK-SIM/FSO communication systems is shown in Fig. 1.

Since the modulated subcarrier signal is sinusoidal having both positive and negative values, a DC bias is added to the MSK signal before it is used to drive the laser diode. This can ensure

that the bias current is always equal to or greater than the threshold current. At the transmitter end, the modulated signal of PPM-MSK-SIM by can be given as

$$s(t) = \sum_{k=1}^L I_k \left[ 1 + \xi \cos \left( \omega_c t + \frac{c_k \pi}{2T_s} t + \varphi_k \right) \cdot g(t - (k-1)T_s) \right] \quad (1)$$

where  $I_k$  is the transmitter irradiance of  $k$ th code element,  $\xi$  is the modulation index,  $\omega_c$  is the angular frequency of the carrier wave,  $c_k$  is codeword of PPM,  $T_s$  is the duration time of one code element,  $\varphi_k$  is the initial phase of  $k$ th code element, and  $g(t)$  is the rectangular pulse shape of one time slot duration.

At the receiver end, the incoming optical radiation need to be filtered firstly through an optical band pass filter (OBPF), then it is converted into electrical signal, which is detected by an APD directly. For the photocurrent is always proportional to the modulated signal, the output instantaneous current for one symbol stream is given by

$$i(t) = RG\alpha \left\{ \sum_{k=1}^L I_k \left[ 1 + \xi \cos \left( \omega_c t + \frac{c_k \pi}{2T_s} t + \varphi_k \right) \cdot g(t - (k-1)T_s) \right] \right\} + n(t) \quad (2)$$

where  $R$  is the photodetector responsivity,  $G$  is the APD average gain,  $\alpha$  is the channel attenuation, and  $n(t)$  is the total receiver noise comprising of thermal noise, and APD shot noise and dark current.

The thermal noise is caused by the thermal fluctuations of electrons in the receiver circuit of equivalent resistance  $R_L$  and temperature  $T$ . Its variance is obtain as [23]

$$\sigma_{th}^2 = \frac{4k_B T F_n}{R_L} \Delta f \quad (3)$$

where  $k_B$  is the Boltzmann constant, and  $F_n$  is the amplifier noise figure, and  $\Delta f$  is the effective noise bandwidth. Here, we use  $\Delta f = R_b/2$ , and  $R_b$  is the system bit rate.

The shot noise is caused by the fluctuation in the received optical power. Then, the instantaneous shot noise can be treated as a stationary Gaussian random process with the variance given by [9]

$$\sigma_{sh}^2 = 2qG^2 F_A R \alpha I \Delta f \quad (4)$$

where  $q$  denotes the electron charge, and  $F_A$  is the excess noise factor.  $F_A$  is given by  $F_A = k_A G + (1 - k_A)(2 - 1/G)$ , where  $k_A$  is the ionization factor [23].

To simplify the analysis, it is assumed that the dark current is negligible. Hence, the variance of the total receiver noise can be expressed as

$$\sigma_n^2 = \sigma_{sh}^2 + \sigma_{th}^2. \quad (5)$$

### 3. Channel Models

During the propagation over atmospheric channel, the modulated optical signal's amplitude and phase are distorted by absorption and scattering from fog, clouds, rain, snow and dust. The link loss consists of geometric loss and atmospheric attenuation. The total channel attenuation is given as [13], [21]

$$\alpha = \frac{A}{\pi \left( \frac{\phi L_d}{2} \right)^2} \exp(-\beta_v L_d) \quad (6)$$

where  $A$ ,  $\beta_v$ ,  $L_d$ , and  $\phi$  are the area of the receiver's aperture, the atmospheric extinction coefficient, the link distance, and the angle of divergence, respectively.

Another major factor that affects the performance of FSO communication is atmospheric turbulence [9]. When the turbulence intensity is weak, we generally use the lognormal turbulence channel to evaluate the performance of the proposed scheme. Thus, the probability density function (PDF) of laser intensity is given as [8], [24]

$$p(I) = \frac{1}{I\sqrt{2\pi\sigma_I^2}} \exp\left\{-\frac{\left(\ln\frac{I}{I_0} + \frac{\sigma_I^2}{2}\right)^2}{2\sigma_I^2}\right\} \quad I \geq 0 \quad (7)$$

where  $I_0$  is the received average irradiance in the absence of turbulence. The parameter  $\sigma_I^2$  is the log intensity variance of turbulences or is called Rytov variance which depends on the channel's characteristics, and assuming plane wave propagation, it is given by [19]

$$\sigma_I^2 = 1.23 C_n^2 k^{\frac{7}{6}} L_d^{\frac{11}{6}} \quad (8)$$

where  $C_n^2$  is the altitude-dependent index of the refractive structure parameter, and  $k$  is the optical wave number.

Assuming  $Z = (I_1 + I_2 + I_3 + \dots + I_N)/I_0 = \exp(U)$  is the sum of  $N$  lognormal random variables with new log intensity variance  $\sigma_Z^2$  and new mean  $u_Z$ , the PDF of  $Z$  is defined as [8]

$$p(Z) = \frac{1}{Z\sqrt{2\pi\sigma_Z^2}} \exp\left\{-\frac{(\ln Z - u_Z)^2}{2\sigma_Z^2}\right\} \quad (9)$$

$$u_Z = \ln(N) - \frac{1}{2} \ln\left[1 + \frac{\exp(\sigma_I^2) - 1}{N}\right] \quad (10)$$

$$\sigma_Z^2 = \ln\left[1 + \frac{\exp(\sigma_I^2) - 1}{N}\right]. \quad (11)$$

#### 4. BER Performance Analysis

In the hybrid PPM-MSK-SIM/FSO systems, to simplify the analysis, let the subcarrier phase is equal to zero, that is,  $\varphi = 0$ . Then, the signal for one symbol period at the sampler output is obtain as

$$i_D(t) = \frac{\xi R G_\alpha}{2} \sum_{k=1}^L I_k + n_D(t) \quad (12)$$

where  $n_D(t)$  is AWGN with variance  $\sigma_{L-PPM}^2/2$ , and  $\sigma_{L-PPM}^2 = N_0 R_b L / (2M)$ , where  $N_0$  is the double-sided power spectral density of the Gaussian noise [13].

Assuming an equivalent probable data transmission, in other words,  $P(1) = P(0) = 0.5$ , the conditional error probability for the received signal becomes

$$P_{ec} = P(1)P_{e1} + P(0)P_{e0}. \quad (13)$$

The marginal probabilities are given by

$$P_{e1} = \int_{-\infty}^0 \frac{1}{\sqrt{2\pi\sigma^2}} \exp\left[-\frac{(i_D(t) - \kappa)^2}{2\sigma^2}\right] di_D(t) \quad (14)$$

$$P_{e0} = \int_0^{+\infty} \frac{1}{\sqrt{2\pi\sigma^2}} \exp\left[-\frac{(i_D(t) + \kappa)^2}{2\sigma^2}\right] di_D(t) \quad (15)$$

where  $\kappa$  is the detection threshold. In order to evaluate the error performance of the hybrid modulation scheme, the BER is calculated for  $L = 2$ . From the apparent symmetry of (14) and (15), the conditional BER for 2-PPM-MSK-SIM for the received signal can be written as

$$P_{ec} = Q\left(\frac{\xi R G \alpha I_0 Z}{\sqrt{2\sigma_{2\text{-PPM}}^2}}\right) \quad (16)$$

where  $Q(x) = \int_x^{+\infty} (1/\sqrt{2\pi}) e^{-t^2/2} dt$ .

Therefore, the unconditional BER for 2-PPM-MSK-SIM is obtained by averaging (16) over the lognormal irradiance fluctuation statistics to be

$$P_e = \int_0^{+\infty} P_{ec} p(Z) dZ. \quad (17)$$

A closed-form solution of (17) does not exist and using the numerical integration could result in truncating its upper limit. Thus, by using the Gauss–Hermite quadrature integration approximation of (18) [22], the analytical difficulty involved solving (17) can be circumvented

$$\int_{-\infty}^{+\infty} f(x) \exp(-x^2) dx = \sum_{i=1}^m w_i f(x_i) \quad (18)$$

where  $w_i$  and  $x_i$  are the weighting factors and the zeros of the Hermite polynomial, respectively.

Then, as proved in the Appendix, we can obtain a tractable expression of  $P_e$ , that is

$$P_e = \frac{1}{\sqrt{\pi}} \sum_{i=1}^m w_i Q\left[\frac{\xi R G \alpha}{2\sqrt{\sigma_{n,i}^2}} I_0 \exp(\sqrt{2}\sigma_z x_i + u_z)\right] \quad (19)$$

with

$$\sigma_{n,i}^2 = 2qG^2 F_A R \alpha I_0 \exp(\sqrt{2}\sigma_z x_i + u_z) \Delta f + \frac{4k_B T F_n}{R_L} \Delta f. \quad (20)$$

## 5. Numerical Results and Discussion

To evaluate the BER performance, it is desirable to compare the PPM-MSK-SIM with PPM and BPSK-SIM schemes via computer simulations. In this section, the analytical and simulation error probabilities are carried out over the lognormal turbulence channels. Unless otherwise noted, the parameters associated with the system model and constants are listed in Table 1.

The BER for 2-PPM-MSK-SIM compared with 2-PPM and BPSK-SIM schemes over the different lognormal turbulence channels is shown in Fig. 2. Whether the strength of turbulence is  $C_n^2 = 2.5 \times 10^{-15} \text{ m}^{-2/3}$  or  $C_n^2 = 7.5 \times 10^{-15} \text{ m}^{-2/3}$ , the consistency of the results of numerical simulation and theoretical analysis are quite good, which shows that our numerical simulation is correct. In addition, we found that the error performance of 2-PPM-MSK-SIM is obviously better than that of 2-PPM and BPSK-SIM. For example, at the same average received irradiance of  $-2.1 \text{ dBm}$  and the same the strength of turbulence  $C_n^2 = 7.5 \times 10^{-15} \text{ m}^{-2/3}$ , the BER performance of 2-PPM-MSK-SIM can decrease to  $1.02 \times 10^{-9}$ , while that of 2-PPM and BPSK-SIM are just  $1.19 \times 10^{-7}$  and  $2.29 \times 10^{-6}$ , respectively. At the same time, this advantage of 2-PPM-MSK-SIM increase gradually compared with 2-PPM and BPSK-SIM as the strength of turbulence increases. For example, when the BER is  $1.0 \times 10^{-9}$ , the average received irradiance required by the 2-PPM-MSK-SIM is less  $2.5 \text{ dBm}$  than by the BPSK-SIM when the strength of turbulence is  $C_n^2 = 2.5 \times 10^{-15} \text{ m}^{-2/3}$ , but this kind of difference is increased to

TABLE 1

List of parameters and constants

Name	Symbol	Value
wavelength	$\lambda$	850 nm
receiver's aperture diameter	$D$	0.04 m
link distance	$L_d$	1000 m
receiver noise temperature	$T$	300 K
APD load resistance	$R_L$	1000 $\Omega$
APD average gain	$G$	10
bit rate	$R_b$	2 Gb/s
responsivity	$R$	1
modulation index	$\xi$	1
amplifier noise figure	$F_n$	2
ionization factor	$k_A$	0.7
atmospheric extinction coefficient	$\beta_v$	0.1 dB/km
angle of divergence	$\phi$	$10^{-3}$ rad
Boltzmann's constant	$k_B$	$1.38 \times 10^{-23}$ W/K/Hz
Electron charge	$q$	$1.69 \times 10^{-19}$ C

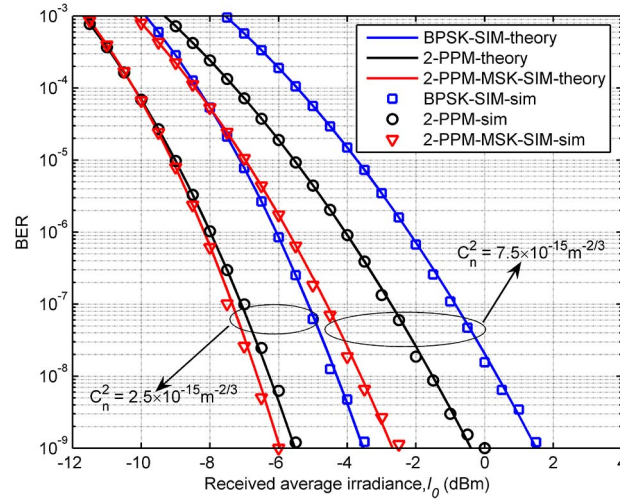


Fig. 2. BER against the average received irradiance for 2-PPM-MSK-SIM, 2-PPM, and BPSK-SIM in the different lognormal turbulence channels.

4.5 dBm when the strength of turbulence is  $C_n^2 = 7.5 \times 10^{-15} \text{ m}^{-2/3}$ . Hence, the PPM-MSK-SIM can significantly improve the system performance over the lognormal turbulence channels. The reasons for these results are that the PPM-MSK-SIM has not only the strong anti-interference of MSK but the high power utilization ratio of PPM as well.

When the average length of symbol  $L$  of PPM-MSK-SIM is changed, its BER performance is shown in Fig. 3. Here,  $L = 4$  and  $C_n^2 = 8.5 \times 10^{-15} \text{ m}^{-2/3}$ . It is also found that the error performance of 4-PPM-MSK-SIM is superior to that of 4-PPM and BPSK-SIM schemes. By comparing the Figs. 2 and 3, we can obtain the conclusion that the inherent advantages of PPM-MSK-SIM compared with PPM and BPSK-SIM will be still maintained with the increase of  $L$ .



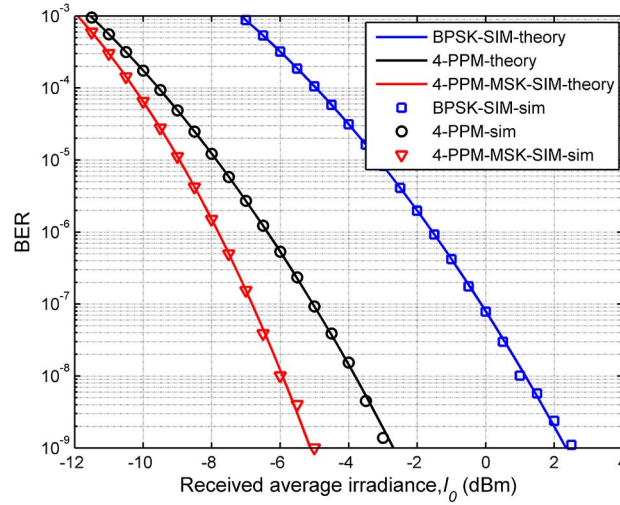


Fig. 3. BER against the average received irradiance for 4-PPM-MSK-SIM, 4-PPM, and BPSK-SIM in the lognormal turbulence channel.

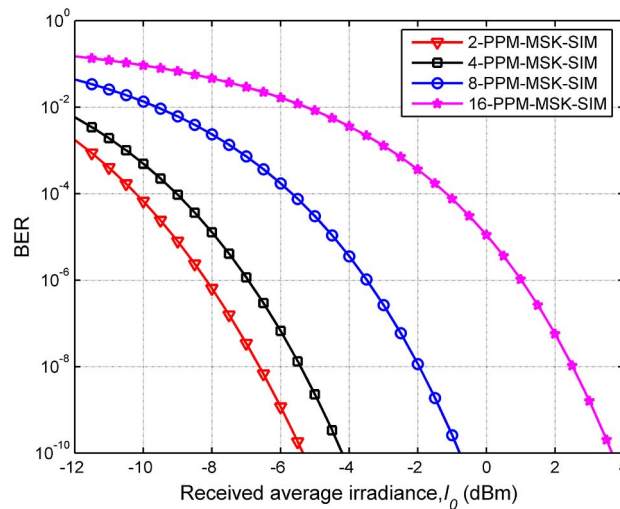


Fig. 4. BER against the received irradiance for 2-, 4-, 8-, and 16-PPM-MSK-SIM in the lognormal turbulence channel for  $C_n^2 = 2.5 \times 10^{-15} \text{ m}^{-2/3}$ .

The BER performance changes with the average length of symbol  $L$  is presented in Fig. 4. With the increase of  $L$ , the BER performance of PPM-MSK-SIM decreases. In this case, the modulation order  $M$  is enlarged with the increase of  $L$ , more and more data are converted from parallel-to-serial at the transmitter end, and a tiny part of them cannot be transmitted effectively; meanwhile, at the receiver end, the data are changed from serial-to-parallel after MSK demodulation, and need be judgment according to the maximal photocurrent in the process of PPM demodulation, this leads to the error probability increase while the average length of symbol  $L$  is enlarged, thus the BER performance of PPM-MSK-SIM decreases accordingly.

With the link distance increase, the system BER of different modulation schemes in the lognormal turbulence channel is shown in Fig. 5. We can also find that the BER performance of 2-PPM-MSK-SIM is obviously better than that of 2-PPM and BPSK-SIM; however, this kind of advantage



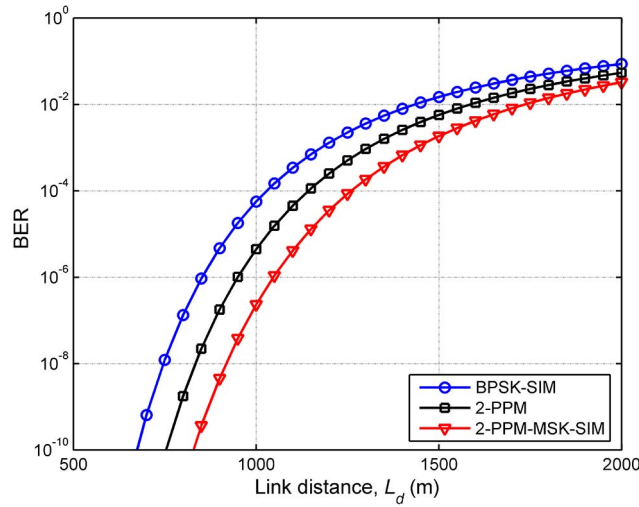


Fig. 5. BER against the link distance for 2-PPM-MSK-SIM, 2-PPM, and BPSK-SIM in the lognormal turbulence channel,  $I_0 = -5$  dBm, and  $C_n^2 = 7.5 \times 10^{-15} \text{ m}^{-2/3}$ .

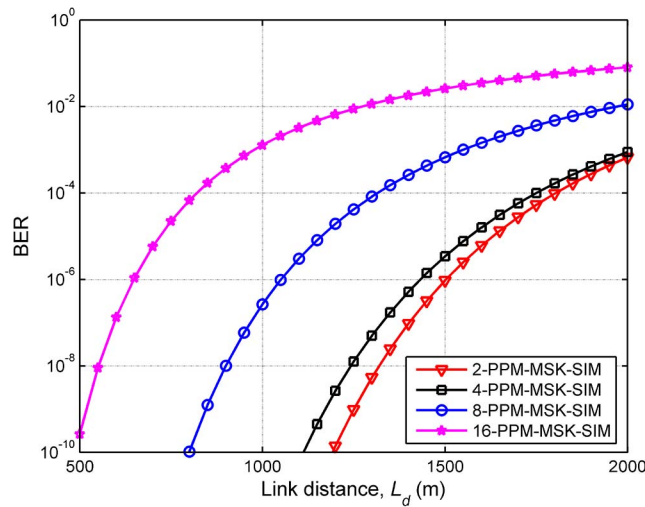


Fig. 6. BER against the link distance for 2-, 4-, 8-, and 16-PPM-MSK-SIM in the lognormal turbulence channel,  $I_0 = -3$  dBm, and  $C_n^2 = 2.5 \times 10^{-15} \text{ m}^{-2/3}$ .

is gradually reduced with the increase of the link distance  $L_d$ . At the same time, the error performance of the system decreases with the increase of the link distance  $L_d$  too. In this case, the increase of link distance is equivalent to enlarging the log intensity variance according to their expression  $\sigma_I^2 = 1.23C_n^2 k^{7/6} L_d^{11/6}$ ; therefore, the larger link distance, the worse BER performance of different modulation schemes.

For different average length of symbol  $L$ , the BER performance of PPM-MSK-SIM changed with the link distance is presented in Fig. 6. As shown, the BER performance of PPM-MSK-SIM decreases monotonously with the increase of the link distance for different  $L$  firstly, but this difference between them is gradually smaller; and moreover, for different  $L$ , its value is bigger, the error performance of PPM-MSK-SIM is worse. Therefore, we can get the conclusion that the BER performance of PPM-MSK-SIM decreases along with the average length of symbol  $L$  increase.

## 6. Conclusion

In this paper, we propose a new hybrid modulation scheme called PPM-MSK-SIM, which is based on PPM and MSK-SIM and combines the advantages of MSK's strong anti-interference and PPM's high power utilization ratio concurrently. Then, its BER performance is investigated in detail over lognormal atmospheric turbulence channels with an APD detector. The results show that the BER performance of PPM-MSK-SIM is obviously better than PPM and BPSK-SIM not only for different average length of symbol  $L$  but also for increased link distance; Particularly, this kind of superiority can be moderately improved as the turbulence increase in the lognormal channel. Moreover, the BER performance of PPM-MSK-SIM schemes for  $L = 2, 4$ , and  $8$  over the lognormal turbulence channels are compared, the research achievement shows that the error performance decreases with the increase of  $L$ . These above considerations make the PPM-MSK-SIM a favorable candidate to select as the modulation technique in FSO communication systems.

## Appendix

### Proof of BER [(19) and (20)]

Substituting (10) and (16) into (17), the unconditional BER for 2-PPM-MSK-SIM over the lognormal irradiance fluctuation statistics is reproduced by

$$P_e = \int_0^{+\infty} P_{ec} p(Z) dZ$$

$$= \int_0^{+\infty} Q\left(\frac{\xi R G \alpha l_0 Z}{\sqrt{2\sigma_{2-PPM}^2}}\right) \cdot \frac{1}{Z \sqrt{2\pi\sigma_z^2}} \exp\left\{-\frac{(\ln Z - u_z)^2}{2\sigma_z^2}\right\} dZ. \quad (A.1)$$

By invoking a change of variable  $x = (\ln Z - u_z)/\sqrt{2}\sigma_z$  and using (18), then the tractable expression of  $P_e$  is

$$P_e = \int_0^{+\infty} Q\left(\frac{\xi R G \alpha l_0}{\sqrt{2\sigma_{2-PPM}^2}} \cdot \exp(\sqrt{2}\sigma_z x + u_z)\right) \cdot \frac{1}{\sqrt{\pi}} \exp\{-x^2\} dx$$

$$= \frac{1}{\sqrt{\pi}} \int_0^{+\infty} Q\left(\frac{\xi R G \alpha l_0}{2\sqrt{\sigma_n^2}} \cdot \exp(\sqrt{2}\sigma_z x + u_z)\right) \cdot \exp\{-x^2\} dx$$

$$= \frac{1}{\sqrt{\pi}} \sum_{i=1}^m w_i Q\left[\frac{\xi R G \alpha}{2\sqrt{\sigma_{n,i}^2}} l_0 \exp(\sqrt{2}\sigma_z x_i + u_z)\right] \quad (A.2)$$

with

$$\sigma_n^2 = 2qG^2 F_A R \alpha l_0 Z \Delta f + \frac{4k_B T F_n}{R_L} \Delta f$$

$$= 2qG^2 F_A R \alpha l_0 \exp(\sqrt{2}\sigma_z x + u_z) \Delta f + \frac{4k_B T F_n}{R_L} \Delta f. \quad (A.3)$$

## References

- [1] V. W. S. Chan, "Free-space optical communications," *J. Lightwave Technol.*, vol. 24, no. 12, pp. 4750–4762, Dec. 2006.
- [2] M. Rouissat, R. A. Borsali, and M. E. Chikh-Bled, "A new modified MPPM for high-speed wireless optical communication systems," *ETRI J.*, vol. 35, no. 2, pp. 188–192, Apr. 2013.

- [3] R. Liao, H. Liu, and Y. Qiao, "New hybrid reverse differential pulse position width modulation scheme for wireless optical communication," *Opt. Eng.*, vol. 53, no. 5, May 2014, Art. ID. 056112.
- [4] K. Wakafuji and T. Ohtsuki, "Performance analysis of atmospheric optical subcarrier-multiplexing systems and atmospheric optical subcarrier-modulated code-division multiplexing systems," *J. Lightwave Technol.*, vol. 23, no. 4, pp. 1676–1682, Apr. 2005.
- [5] A. K. Majumdar, "Free-space laser communication performance in the atmospheric channel," *J. Opt. Fiber Commun. Rep.*, vol. 2, no. 4, pp. 345–396, Oct. 2005.
- [6] M. Niu, X. Song, J. Cheng, and J. F. Holzman, "Performance analysis of coherent wireless optical communications with atmospheric turbulence," *Opt. Express*, vol. 20, no. 6, pp. 6515–6520, Mar. 12, 2012.
- [7] S. Karp, R. M. Gagliardi, S. E. Moran, and L. B. Stotts, *Optical Channels: Fibers, Clouds, Water, and the Atmosphere*, New York, NY, USA: Plenum, 1988.
- [8] X. Zhu and J. M. Kahn, "Free-space optical communication through atmospheric turbulence channels," *IEEE Trans. Commun.*, vol. 50, no. 8, pp. 1293–1300, Aug. 2002.
- [9] D. A. Luong, A. T. Pham, and T. C. Thang, "Effect of avalanche photodiode and thermal noises on the performance of binary phase-shift keying-subcarrier-intensity modulation/free-space optical systems over turbulence channels," *IET Commun.*, vol. 7, no. 8, pp. 738–744, May 2013.
- [10] J. Li, J. Q. Liu, and D. P. Taylor, "Optical communication using subcarrier PSK intensity modulation through atmospheric turbulence channels," *IEEE Trans. Commun.*, vol. 55, no. 8, pp. 1598–1606, Aug. 2007.
- [11] W. O. Popoola and Z. Ghassemlooy, "BPSK subcarrier intensity modulated free-space optical communications in atmospheric turbulence," *J. Lightwave Technol.*, vol. 27, no. 8, pp. 967–973, Apr. 15, 2009.
- [12] W. Lim, C. Yun, and K. Kim, "BER performance analysis of radio over free-space optical systems considering laser phase noise under Gamma-Gamma turbulence channels," *Opt. Express*, vol. 17, no. 6, pp. 4479–4484, Mar. 16, 2009.
- [13] J. R. Barry, *Wireless Infrared Communications*. New York, NY, USA: Springer-Verlag, 1994.
- [14] H.-H. Chan, K. L. Sterckx, J. M. Elmirghani, and R. A. Cryan, "Performance of optical wireless OOK and PPM systems under the constraints of ambient noise and multipath dispersion," *IEEE Commun. Mag.*, vol. 36, no. 12, pp. 83–87, Dec. 1998.
- [15] J. Ma, Y. Jiang, S. Yu, L. Tan, and W. Du, "Packet error rate analysis of OOK, DPIM and PPM modulation schemes for ground-to-satellite optical communications," *Opt. Commun.*, vol. 283, no. 2, pp. 237–242, Jan. 2010.
- [16] W. Huang, J. Takayanagi, T. Sakanaka, and M. Nakagawa, "Atmospheric optical communication system using subcarrier PSK modulation," *IEICE Trans. Commun.*, vol. 76, no. 9, pp. 1169–1177, Sep. 1993.
- [17] W. O. Popoola, Z. Ghassemlooy, S. Gao, J. I. H. Allen, and E. Leitgeb, "Free-space optical communication employing subcarrier modulation and spatial diversity in atmospheric turbulence channel," *IET Optoelectron.*, vol. 2, no. 1, pp. 16–23, Feb. 2008.
- [18] X. Song and J. Cheng, "Subcarrier intensity modulated optical wireless communications using noncoherent and differentially coherent modulations," *J. Lightwave Technol.*, vol. 31, no. 12, pp. 1906–1913, Jun. 15, 2013.
- [19] M. Faridzadeh, A. Gholami, Z. Ghassemlooy, and S. Rajbhandari, "Hybrid pulse position modulation and binary phase shift keying subcarrier intensity modulation for free space optics in a weak and saturated turbulence channel," *J. Opt. Soc. Amer. A*, vol. 29, no. 8, pp. 1680–1685, Aug. 2012.
- [20] K. Prabhu, S. Bose, and D. Sriram Kumar, "BPSK based subcarrier intensity modulated free space optical system in combined strong atmospheric turbulence," *Opt. Commun.*, vol. 305, pp. 185–189, Sep. 2013.
- [21] B. R. Strickland, M. J. Lavan, E. Woodbridge, and V. Chan, "Effects of fog on the bit-error rate of a free-space laser communication system," *Appl. Opt.*, vol. 38, no. 3, pp. 424–431, Jan. 1999.
- [22] Z. Ghassemlooy, W. Popoola, and S. Rajbhandari, *Optical Wireless Communications: System and Channel Modeling with MATLAB*. New York, NY, USA: CRC, 2012.
- [23] K. Kiasaleh, "Performance of APD-based, PPM free-space optical communication systems in atmospheric turbulence," *IEEE Trans. Commun.*, vol. 53, no. 9, pp. 1455–1461, Sep. 2005.
- [24] J. Ding, M. Li, M. Tang, Y. Li, and Y. Song, "BER performance of MSK in ground-to-satellite uplink optical communication under the influence of atmospheric turbulence and detector noise," *Opt. Lett.*, vol. 38, no. 18, pp. 3488–3491, Sep. 15, 2013.